Available online at www.sciencedirect.com
SCIENCE DIRECT®

Journal of the European Ceramic Society 23 (2003) 1375–1381

www.elsevier.com/locate/jeurceramsoc

Thermal decomposition products of the heteronuclear complex, $LaNi(dhbaen)(NO_3)(H_2O)_n$

Hiromichi Aono[a], Nobuyuki Kondo[b], Masatomi Sakamoto[b], Enrico Traversa[c], Yoshihiko Sadaoka[a,*]

[a]*Department of Materials Science and Engineering, Faculty of Engineering, Ehime University, Matsuyama 790-8577, Japan*
[b]*Department of Material and Biological Chemistry, Faculty of Science, Yamagata University, Yamagata 990-8560, Japan*
[c]*Department of Chemical Science and Technology, University of Roma "Tor Vergata", 00133 Rome, Italy*

Received 8 February 2002; accepted 16 September 2002

Abstract

The heteronuclear $LaNi(dhbaen)(NO_3)(H_2O)_n$ complex was synthesized and its thermal decomposition products were analyzed by differential thermal analysis (TG/DTA), X-ray diffraction (XRD), Fourier-transform infrared (FT-IR) spectroscopy, Auger electron spectroscopy (AES) with scanning electron microscopy (SEM), and transmission electron microscopy (TEM). Hexagonal perovskite-type $LaNiO_3$ having fine particle size was obtained by sintering at 600 °C. AES showed that the elemental distributions of La, Ni, and O on the surface were very homogeneous for the sample decomposed at 900 °C. The $LaNiO_3$ decomposed to $La_3Ni_2O_7$ and NiO when the heating temperature increases up to 1000 °C. Heteronuclear $LnNi(dhbaen)(NO_3)(H_2O)_n$ complexes (with Ln = Pr, Nd, Sm, and Gd) were also synthesized. The perovskite-type $LnNiO_3$ phase could not be formed by their thermal decomposition.

Keywords: Calcination; $LaNiO_3$; Phase development; Precursors: organic

1. Introduction

Perovskite-type oxides ($LnMO_3$, Ln = lanthanoid and M = transition metal) have useful functional properties and have been investigated for many applications such as catalysts,[1] fuel cells,[2] solid electrolytes,[3] and gas sensors.[4–11] Amongst these oxides, compounds of the $LnNiO_3$ family are promising for applications as catalysts and cathode materials for solid oxide fuel cells (SOFC).[12]

The conventional method of heterometallic oxide production involves a solid-state reaction of the corresponding single oxides. However, the preparation of $LnNiO_3$ single phases is difficult using the solid-state reaction because these phases are not stable at high temperatures.[12,13] In addition, powder materials with controlled stoichiometry and microstructure are needed for these applications. Chemical processing methods can be used to obtain better control of powder quality and microstructure. For these reasons, $LnNiO_3$ compounds have been prepared by chemical synthesis at low temperatures with methods such as sol-gel and coprecipitation.[14,15]

The thermal decomposition of heteronuclear complexes is a promising method for the preparation of di- or tri-metallic oxides, as previously proposed by the authors of this paper.[16] Homogeneous heterometallic oxides with relatively high specific surface area are formed at low temperatures when heteronuclear complexes were used as precursors.[17–28] The synthesis of a LaNi-heteronuclear $LaNi(dhbaen)(NO_3)(H_2O)_n$ complex, where dhbaen is *N*,*N*′-bis (3-hydroxysalicylidene)-ethylenediamine, has been reported in the literature together with the study of its crystal structure.[29,30] Then, the synthesis of $LnNi(dhbaen)(NO_3)(H_2O)_n$, with Ln = La, Eu, or Gd, complexes has been also reported by some of the authors of this paper.[31] However, the thermal decomposition products of the $LaNi(dhbaen)(NO_3)(H_2O)_n$ complex have not been investigated in detail yet.[32] Moreover, the thermal decomposition of the other

* Corresponding author. Tel.: +81-89-927-9891; fax: +81-89-927-9856.
E-mail address: sadaoka@eng.2.ehime-u.ac.jp (Y. Sadaoka).

0955-2219/03/$ - see front matter © 2003 Elsevier Science Ltd. All rights reserved.
PII: S0955-2219(02)00350-3

LnNi-complexes such as LnNi(dhbaen)$(NO_3)(H_2O)_n$, with Ln = Pr, Nd, Sm, and Gd, has not been studied at all.

In this paper, we report the synthesis of LnNi(dhbaen)$(NO_3)(H_2O)_n$ complexes (Ln = La, Pr, Nd, Sm, and Gd) and the study of the products of their thermal decomposition. Perovskite-type single phases could be obtained only from the decomposition of the LaNi-complex.

2. Experimental procedure

2.1. Materials preparation

The lanthanoid-nickel heteronuclear complexes were synthesized according to our previously reported method.[31] To prepare a mononuclear Ni(II) complex, [Ni(H_2dhbaen)], an aqueous solution (50 cm^3) of $Ni(CH_3COO)_2 \cdot 4H_2O$ (10 mmol) and then ethylenediamine (10 mmol) were added to a solution of 2,3-dihydroxybenzaldehyde (20 mmol) in methanol (60 cm^3). After the mixture was stirred at room temperature for 2 h, brownish red [Ni(H_2dhbaen)] crystals were collected by suction filtration, washed subsequently with water, methanol and diethylether, and then dried under reduced pressure. A methanolic solution (6 cm^3) of lithium hydroxide monohydrate (3 mmol) was added to a suspension of the synthesized mononuclear Ni(II) complex (1.5 mmol) in methanol (30 cm^3). The mixture was stirred for 1 h at room temperature and hydrated lanthanoid (La, Pr, Nd, Sm, or Gd) nitrate (1.5 mmol) in methanol (3 cm^3) was added. After the mixture was kept warm under stirring for 3 h, brownish yellow microcrystals were collected by suction filtration, washed with methanol and diethylether, and then dried under vacuum. Elemental analyses were carried out at the Instrumental Analysis Center of Chemistry, Faculty of Science, Tohoku University, Japan. C, H, and N elemental contents in the complex were determined by measuring CO_2, H_2O, and NO_2 concentrations in the gas formed from the decomposition of the complex at elevated temperatures.

The complexes were decomposed upon heating at selected temperatures in ambient air for 1 h to obtain the oxide samples.

2.2. Materials analysis

The thermal decomposition behavior of the heteronuclear complexes was examined by simultaneous thermogravimetric and differential thermal analysis (TG/DTA, Seiko Instrument TG/DTA 32), performed with a heating rate of 5 °C/min in air flow. The results of TG/DTA were used to select the heating temperatures for the complex decomposition. X-ray diffraction (XRD, Cu-K_α radiation, Rint 2000, Rigaku, sweep rate 2°/min. 40 kV, 20 mA) analysis was used to study the phases present in the decomposition products. Fourier-transform infrared (FT-IR) absorption spectroscopy (JASCO, FT/IR-600) was used to analyze the functional groups present on the surface of the decomposed samples. Particle size and morphology were evaluated by transmission electron microscopy (TEM, Jeol JEM-100cx) (Bright field image) at an accelerating voltage of 100 kV (camera length of 600 mm). The surface elemental distribution of La, Ni, and O for the decomposed powders were characterized by Auger electron spectroscopy (AES, Perkin-Elmer Phi 650) using the La(MNN), Ni(LMM), and O(KLL) lines, at a voltage of the incident electron beam of 5 kV. Before AES measurement, the powders were pressed into pellets at a pressure of 1×10^8 Pa and then sputtered with Ar gas for 20 min to remove the surface contaminants before the measurements.

3. Results and discussion

3.1. Characterization of the LaNi-complex

The results of elemental analyses for C(32.47%), H(2.72%), and N(7.10%) were in good agreement with the theoretical values estimated to be 32.23% for C, 2.83% for H, and 7.04% for N, for the LaNi(dhbaen)$(NO_3)(H_2O)_2$ complex with 2 molecules of hydration water. Fig. 1 shows the TG/DTA curves for the LaNi-complex. All the measurements performed showed that dehydration started below 50 °C and a plateau was observed in the temperature range 150–230 °C. The weight was ca. 93 wt.% which agreed with the theore-

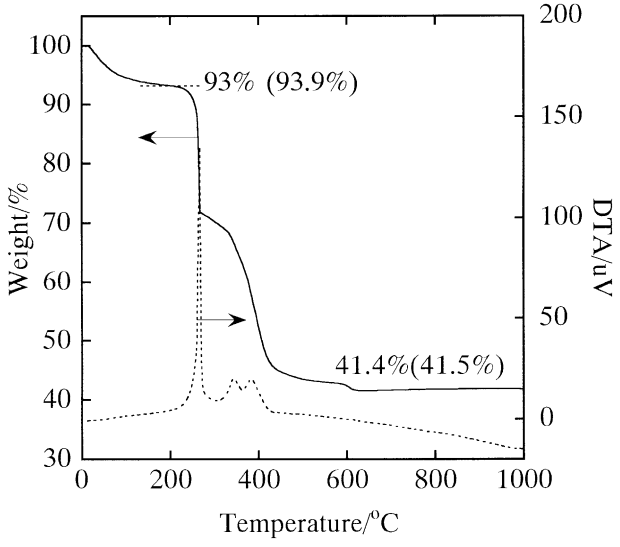

Fig. 1. The TG/DTA curves for the LaNi-complex, at a heating rate of 5 °C/min in air.

tical value of 93.9% caused by the loss of two molecules of crystallization water. The TG curve showed an abrupt weight loss at around 300 °C followed by a slower loss that ended at about 600 °C, accompanied by exothermic effects, as shown by the DTA curve, which can be attributed to the decomposition of the ligand. The weight percentage 41.4 wt.% measured in the last plateau range was in good agreement with the theoretical value of 41.5 wt.%, calculated by assuming the formation of $LaNiO_3$ from the complex with two molecules of water tied up in the crystallization. From these results, the complexes were estimated to be LnNi(dhbaen)$(NO_3)(H_2O)_2$ (Fig. 2).

3.2. Thermal decomposition process for the LaNi-complexes

Fig. 3 shows the XRD powder diffraction patterns for the products of the decomposition of the LaNi-complex at various temperatures. The XRD patterns for the samples fired at 500 °C showed broad peaks of NiO and La_2CO_5 and contained no $LaNiO_3$ peaks. The peaks of the perovskite-type phase were observed for samples decomposed at 600 °C, although small peaks of NiO and La_2CO_5 were still present in the XRD patterns. Only $LaNiO_3$ peaks were detected for samples decomposed in the 700–900 °C temperature range. It is confirmed that the full-width-at-half-maximum (FWHM) of all the $LaNiO_3$ peaks decreases with an increase in decomposition temperature until 900 °C because of crystallite growth. The XRD peaks for $LaNiO_3$ were indexed with hexagonal phase (space group: $R\bar{3}$-c). The lattice constants were $a = b = 0.5434$ nm and $c = 1.3111$ nm for the sample sintered at 900 °C. The $LaNiO_3$ decomposed to a mixture of $La_3Ni_2O_7$ and NiO due to Ni(III) reduction into Ni(II) when the decomposition

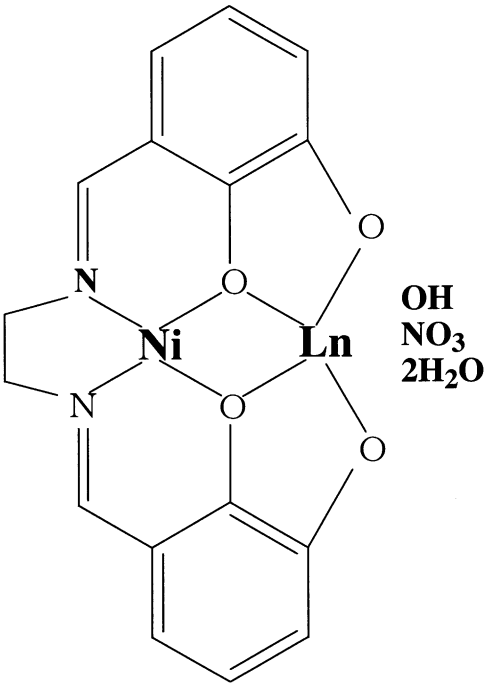

Fig. 2. LnNi(dhbaen)$(NO_3)(H_2O)_4$ complex.

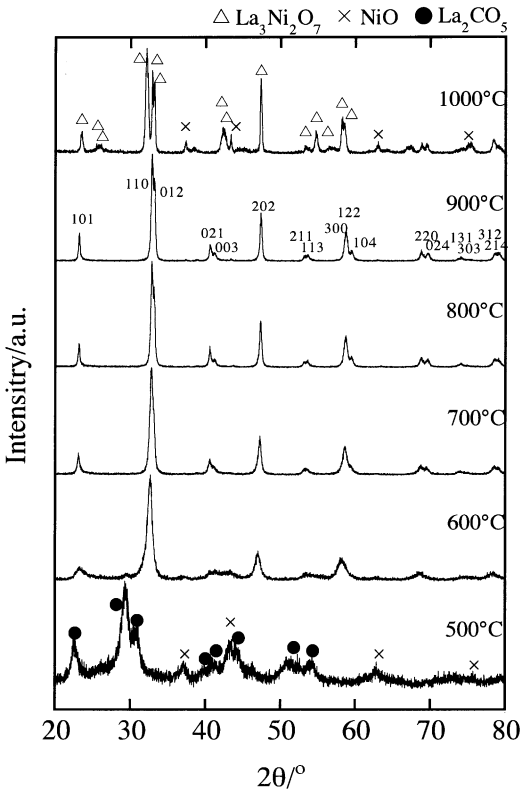

Fig. 3. XRD powder diffraction patterns for the LaNi-complex decomposed at selected temperatures. Decomposition temperatures in °C are shown in the figure. hkl values (hexagonal: $R\bar{3}c$) are shown for the sample sintered at 900 °C.

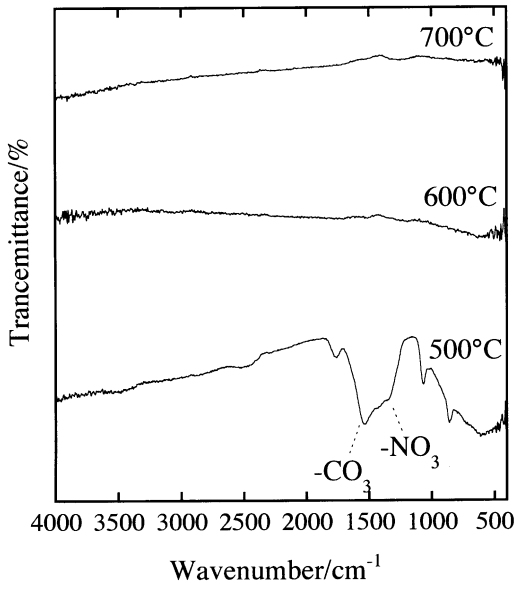

Fig. 4. FT-IR spectra for the LaNi-complex decomposed at various temperatures. Decomposition temperatures in °C are shown in the figure.

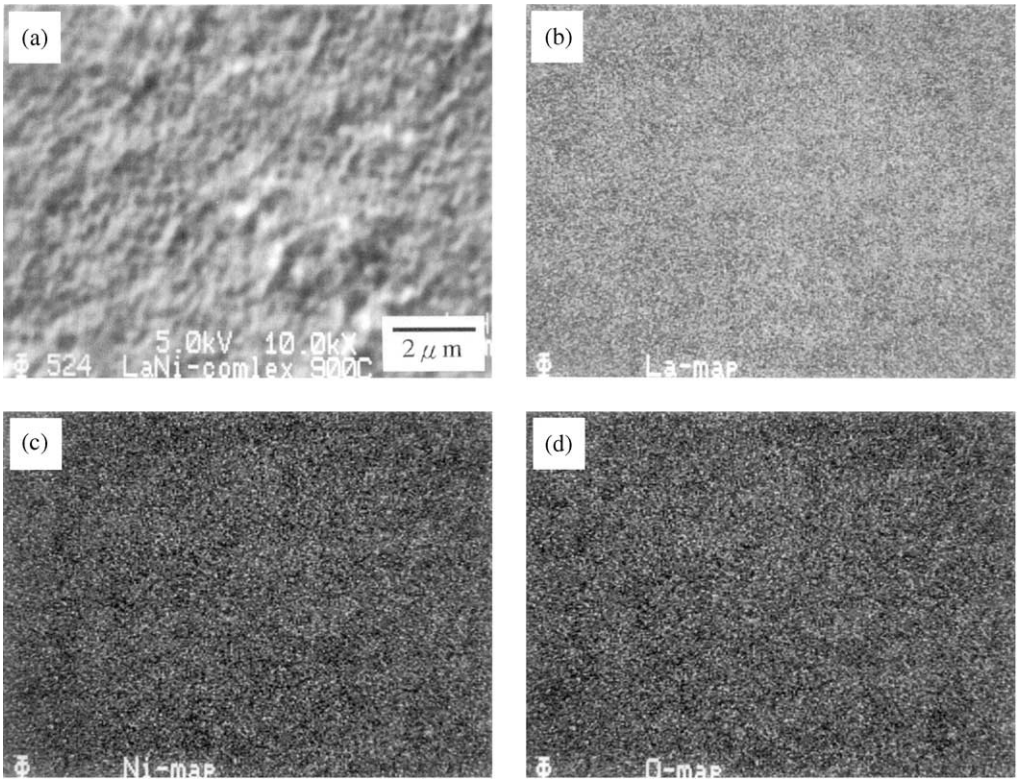

Fig. 5. SEM-Auger results for the LaNi-complex decomposed at 900 °C for 1 h. White and black spots in the Auger results represent the high and low concentrations of each analytical element: (a) SEM, (b) La map, (c) Ni map, (d) O map.

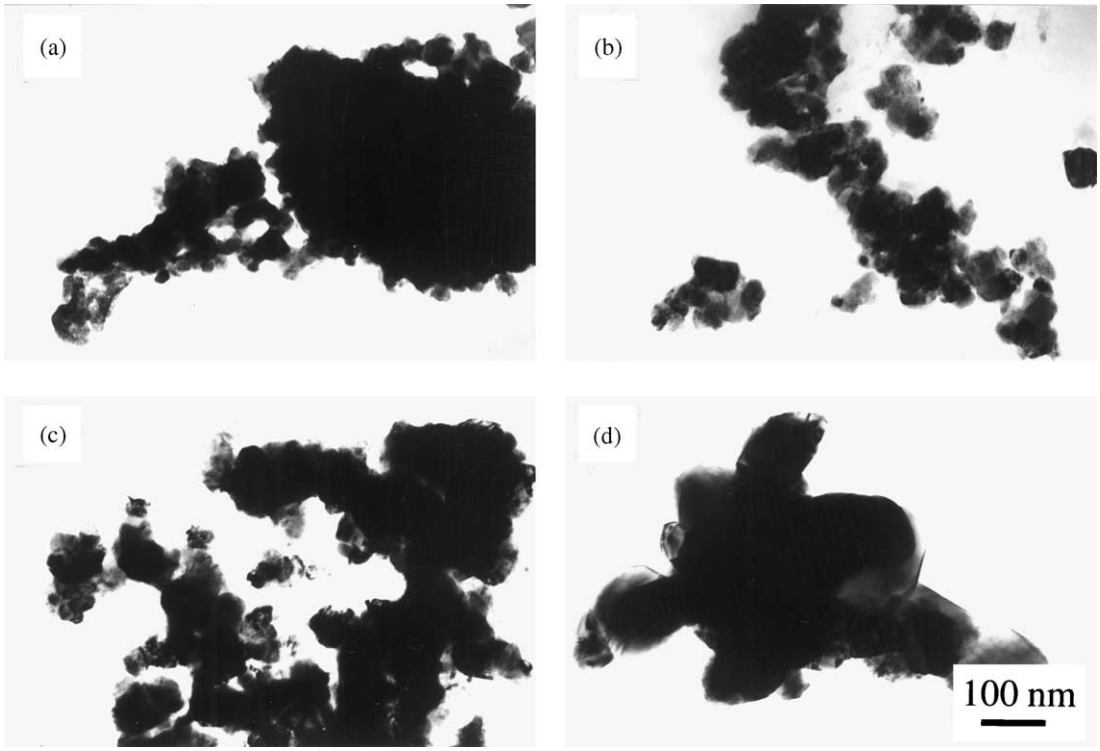

Fig. 6. Bright field TEM micrograph at an accelerating voltage of 100 kV (camera length of 600 mm) for the LaNi-complex decomposed at (a) 600 °C, (b) 700 °C, (c) 800 °C, (d) 900 °C.

temperature increased up to 1000 °C. This decomposition at high temperature has been reported for similar Ni-containing perovskite-type materials.[33]

Fig. 4 shows the FT-IR results for the decomposed LaNi-complex samples. Signal peaks attributable to carbonate and nitrate groups were observed at 1400 and 1500 cm^{-1} for the samples decomposed at 500 °C. Those signals disappeared for the samples decomposed at 600 °C. Therefore, one can conclude that the carbonate and nitrate groups formed by the thermal decomposition of the complex remained at the surface of the perovskite-type oxide grains for the sample decomposed at 500 °C.

Fig. 5 shows the SEM-Auger results for the surface of the $LaNiO_3$ pellet prepared by using the powder obtained by the complex decomposition at 900 °C for 1 h. In the case of the AES measurement, the elemental analysis is very sensitive, because the detectable depth on the surface is around 1 nm. Elemental analyses were operated on the same surface observed by SEM and shown in Fig. 5a. The elemental distribution of La, Ni, and O on the surface was highly homogeneous (Fig. 5b, c, and d, respectively). It is assumed that the thermal decomposition of the heteronuclear complex is a process suitable to prepare single-phase, homogeneous perovskite-type $LaNiO_3$ powders at a temperature as low as 600 °C.

3.3. LnNi-complexes, Ln = Pr, Nd, Sm, or Gd

The results of elemental analyses and TGA for the other LnNi-complexes (Ln = Pr, Nd, Sm or Gd) were in agreement with the theoretical values for complexes containing two molecules of hydration water, thereby confirming the chemical structure and composition of the complexes, as reported above for the LaNi-complex.

However, the thermal decomposition behaviour of the LnNi-complexes was different from what observed for the LaNi-complex. In the case of the NdNi-complex, the decomposition product was a mixture of Nd_2NiO_4 and NiO. The perovskite-type phase was not obtained at any temperature. For the Ln = Pr, Sm and Gd systems, heating the complexes led to a mixture of NiO and Ln_2O_3 (Pr_6O_{11} for Pr) without formation of any polymetallic oxide. For these complexes, the decomposition products did not change even when sintered at 1000 °C.

It should be emphasized that while $LaNiO_3$ samples have been synthesized by chemical processing methods at low temperatures in ambient air, in the case of other LnNi oxides the perovskite-type phase could be synthesized only at high oxygen pressure.[34] The thermal stability of the perovskite phase becomes lower with a decrease in ionic radius, since the perovskite structure distorts from the ideal structure, as shown by the tolerance factors for the $LnNiO_3$ phases reported in Table 1. Table 1 shows also the decomposition products obtained at 900 °C for the tested complexes, and the ionic radius for Ln^{3+} ions.[35] Although the ionic radius of Pr^{3+} ion is larger than that of Nd^{3+}, polymetallic oxides were not obtained because trivalent Pr^{3+} ion is less stable than tetravalent Pr^{4+} ion.

Table 1
Decomposition products at 900 °C, ionic radius for Ln ions, and tolerance factor (t)[a] for $LnNiO_3$

Complex	Decomposition products	IR (Å)	t
$LaNi(dhbaen)(NO_3)(H_2O)_2$	$LaNiO_3$	0.116	0.905
$PrNi(dhbaen)(NO_3)(H_2O)_2$	Pr_6O_{11}, NiO	0.1126	0.893
$NdNi(dhbaen)(NO_3)(H_2O)_2$	Nd_2NiO_4, NiO	0.1109	0.887
$SmNi(dhbaen)(NO_3)(H_2O)_2$	Sm_2O_3, NiO	0.1079	0.876
$GdNi(dhbaen)(NO_3)(H_2O)_2$	Gd_2O_3, NiO	0.1053	0.867

[a] Tolerance factor (t) was calculated using $t = (A + O)/\left[\sqrt{2}(B + O)\right]$, where A, B, O were ionic radius of La^{3+} (see this table), Ni^{3+} (0.060 nm), O^{2-} (0.140 nm), respectively.

3.4. Morphology of $LaNiO_3$ samples

It is of paramount importance to characterize the microstructure of the powders obtained, given that it is well known that many oxide properties such as the catalytic activity and the gas sensing characteristics are strongly influenced by particle size.[36–38] Fig. 6 shows bright field TEM photographs for the LaNi-complex samples decomposed at 600, 700, 800, and 900 °C for 1 h. The average particle size was estimated to be about 20, 30–40, 50, and 100 nm for the samples decomposed at 600 °C (Fig. 6a), 700 °C (Fig. 6b), 800 °C (Fig. 6c), and 900 °C (Fig. 6d), respectively.

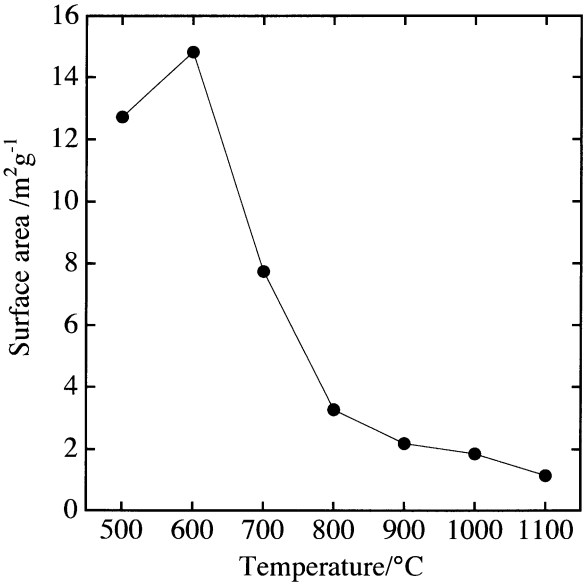

Fig. 7. The relationship between decomposition temperature and specific surface area for the decomposed LaNi-complex samples.

Fig. 7 shows the influence of the heating temperature on the powder specific surface area for the decomposed samples. The specific surface area decreased with an increase in the decomposition temperature above 600 °C, being 14.8 and 7.7 $m^2\ g^{-1}$ for the samples decomposed at 600 and 700 °C, respectively. These values were smaller than the calculated theoretical values, around 43 and around 30 $m^2\ g^{-1}$, assuming the particle shape to be spherical. This should be ascribed to agglomeration and/or necking of particles (see Fig. 6), given that the difference with the theoretical value decreased with increasing the decomposition temperature.

4. Conclusions

Hexagonal $LaNiO_3$ powders having nano-sized particles were prepared by the thermal decomposition at low temperatures of the synthesized heteronuclear complex. These characteristics make these $LaNiO_3$ powders very promising for the application as electroceramics materials. In particular, a good processability to form thick-film coatings is expected for these powders, attractive for applications such as electrodes of SOFCs and chemical sensors.

Acknowledgements

Thanks are due to the Center for Cooperative Research and Development, Ehime University, for the XRD measurements.

References

1. McCarty, J. G. and Wise, H., Perovskite catalysts for methan combustion. *Catalysis Today*, 1990, **8**, 231–248.
2. Minh, N. Q., Ceramic fuel cells. *J. Am. Ceram. Soc.*, 1993, **76**, 563–588.
3. Inaguma, Y., Chen, L., Itoh, M. and Nakamura, T., Candidate compounds with perovskite structure for high lithium ionic conductivity. *Solid State Ionics*, 1994, **70/71**, 196–202.
4. Arakawa, T., Kurachi, H. and Shiokawa, J., Physicochemical properties of rare earth perovskite oxide used as gas sensor material. *J. Mater. Sci.*, 1985, **4**, 1207–1210.
5. Shimizu, Y., Shimabukuro, M., Arai, H. and Seiyama, T., Enhancement of humidity sensitivity for perovskite-type oxides having semiconductivity. *Chem. Lett., 1995, 917–920.*
6. Arakawa, T., Takada, K., Tsunemine, Y. and Shiokawa, J., Carbon monoxide gas sensitivities of reduced perovskite oxide lanthanum cobalt oxide ($LaCoO_{3-x}$). *Sensors and Actuators*, 1988, **14**, 215–221.
7. Matsuura, Y., Matsushima, S., Sakamoto, M. and Sadaoka, Y, NO_2-sensitive $LaFeO_3$ film prepared by thermal decomposition of the heteronuclear complex, $\{La[Fe(CN)_6]\cdot 5H_2O\}_x$. *J. Mater. Chem.*, 1993, **3**, 767–769.
8. Traversa, E., Matsushima, S., Okada, G., Sadaoka, Y., Sakai, Y. and Watanabe, K., NO_2 sensitive $LaFeO_3$ thin films prepared by R.F. Sputtering. *Sensors and Actuators B*, 1995, **24/25**, 661–664.
9. Traversa, E., Villanti, S., Gusmano, G., Aono, H. and Sadaoka, Y., Design of ceramic materials for chemical sensors: $SmFeO_3$ thick films sensitive to NO_2. *J. Am. Ceram. Soc.*, 1999, **82**, 2442–2450.
10. Aono, H., Ohmori, J. and Sadaoka, Y, Effects of sintering atmosphere on surface structure and electrical properties of $LaFeO_3$ prepared by thermal decomposition of La[Fe(CN)$_6$][?0-x81?]E4H_2O. *J. Ceram. Soc. Jpn.*, 2000, **108**, 892–897.
11. Aono, H., Sato, M., Traversa, E., Sakamoto, M. and Sadaoka, Y., Design of ceramic materials for chemical sensors: effect of $SmFeO_3$ processing on its surface and electrical properties. *J. Am. Ceram. Soc.*, 2001, **84**, 341–347.
12. Matsumoto, Y., Yoneyama, H. and Tamura, H., A new catalyst for cathodic reduction of oxygen: lanthanum nickel oxide. *Chem. Lett.*, 1975, 661–662.
13. Park, I. and Lee, H., Thermal stability and reducibility of perovskite-type mixed oxide $LaBO_3$ (B = Fe, Co, Ni). *Bull. Korean Chem. Soc.*, 1988, **9**(5), 283–288.
14. Radhakrishna, I., Nagarajarao, K. and Lakshmanan, A., Preparation of lanthanum nickelate powder by the sol-gel method. *Bulletin of Electrochemistry*, 1993, **9**, 324–535.
15. Singh, R. N., Jain, A. N., Tiwari, S. K., Poillerat, G. and Chartier, P., Physicochemical and electrocatalytic properties of $LaNiO_3$ prepared by a low-temperature route for anode application in alkaline water electrolytsis. *J. Applied Electrochem.*, 1995, **25**, 1133–1138.
16. Traversa, E., Sakamoto, M. and Sadaoka, Y., A chemical route for the preparation of nanosized rare earth perovskite-type oxides for electroceramic applications. *Particulate Sci. Technol.*, 1998, **16**, 185–214.
17. Sadaoka, Y., Watanabe, K., Sakai, Y. and Sakamoto, M., Preparation of perovskite-type oxides by thermal decomposition of heteronuclear complexes, $\{Ln[Fe(CN)_6].nH_2O\}_x$, (Ln = La ~ Ho). *J. Alloys Comp.*, 1995, **224**, 194–198.
18. Sadaoka, Y., Watanabe, K., Sakai, Y. and Sakamoto, M., Thermal decomposition behavior of heteronuclear complexes, $Ln[Co(CN)_6].nH_2O$ (Ln = La-Yb). *J. Ceram. Soc. Jpn.*, 1995, **103**, 519–522.
19. Traversa, E., Sakamoto, M. and Sadaoka, Y., Mechanism of $LaFeO_3$ perovskite-type oxide formation from the thermal decomposition of *d-f* heteronuclear complex, $La[Fe(CN)_6]\cdot 5H_2O$. *J. Am. Ceram. Soc.*, 1996, **79**, 1401–1404.
20. Sadaoka, Y., Traversa, E. and Sakamoto, M., Preparation and structural characterization of perovskite-type $La_xLn''_{1-x}CoO_3$ by the thermal decomposition of heteronuclear complexes, $La_xLn''_{1-x}[Co(CN)_6]\cdot nH_2O$ (Ln'' = Sm and Ho). *J. Alloys Comp.*, 1996, **240**, 51–59.
21. Sadaoka, Y., Traversa, E. and Sakamoto, M., Preparation and characterization of perovskite-type $Ln'_xLn''_{1-x}CoO_3$ for electroceramic applications. *J. Mater. Chem.*, 1996, **6**, 1355–1360.
22. Sakamoto, M., Nunziante, P., Traversa, E., Matsushima, S., Miwa, M., Aono, H. and Sadaoka, Y., Preparation of perovskite-type oxides by the thermal decomposition of heteronuclear complexes, $Ln[Fe_XCo_{1-X}(CN)_6]\cdot 4H_2O$ (Ln = Pr ~ Yb). *J. Ceram. Soc. Jpn.*, 1997, **105[11]**, 963–969.
23. Sakamoto, M., Igoshi, T., Sato, M., Matsushima, S., Miwa, M., Aono, H. and Sadaoka, Y., Thermal decomposition products of heteronuclear Cu-RE complexes, $CuRE(dhbaen)(NO_3)\cdot nH_2O$ (RE = La, Eu, Gd, Tb, Dy, Y, Ho, Er, Tm, Yb, and Lu). *J. Alloys Comp.*, 1997, **260**, 59–63.
24. Sadaoka, Y., Aono, H., Traversa, E. and Sakamoto, M., Thermal evolution of nanosized $LaFeO_3$ powders from a heteronuclear complex, $La[Fe(CN)_6]\cdot nH_2O$. *J. Alloys Comp.*, 1998, **278**, 135–141.
25. Aono, H., Kinoshita, K., Sadaoka, Y. and Sakamoto, M., Characterizations of $NdFe_{0.5}Co_{0.5}O_3$ trimetallic oxide prepared by thermal decomposition of heteronuclear complex, $Nd[Fe_{0.5}Co_{0.5}(CN)_6]\cdot 4H_2O$. *J. Ceram. Soc. Jpn.*, 1998, **106**(10), 958–963.

26. Hasegawa, E., Aono, H., Igoshi, T., Sakamoto, M., Traversa, E. and Sadaoka, Y., Preparation of $YBa_2Cu_3O_{7-\delta}$ powders by the thermal decomposition of a heteronuclear complex, $CuY_{1/3}Ba_{2/3}(dhbaen)(NO_3)_{1/3}(H_2O)_3$. *J. Alloys Comp*., 1999, **287**, 150–158.
27. Aono, H., Tsuzaki, M., Kawaura, A., Sakamoto, M., Traversa, E. and Sadaoka, Y., Preparation of nanosized perovskite-type $LaMnO_3$ powders using the thermal decomposition of a heteronuclear complex, $LaMn(dhbaen)(OH)(NO_3)(H_2O)_4$. *J. Am. Ceram. Soc*., 2001, **84**(5), 969–975.
28. Aono, H., Sakamoto, M. and Sadaoka, Y., Thermally decomposed products of heteronuclear complexes, $CuRE(dhbaen)(NO_3)(dmso)_m(H_2O)_n$, (RE = Sm, Eu, Gd, Tb, Dy, Y, Ho, Er, Tm, Tb, and Lu). *J. Ceram. Soc. Jpn*., 2001, **109**(5), 419–424.
29. Casellato, U., Guerriero, P., Tamburini, S., Sitran, S. and Vigato, P. A., From compounds to materials: heterodinuclear complexes as precursors in the synthesis of mixed oxides; crystal structures of $[Cu(H_2L_A)]$ and $[\{CuY(L_A)(NO_3)(dmso)\}_2]\cdot 2dmso$ [H_4L_A = N,N′-ethylenebis(3-hydroxysalicylideneimine), dmso = dimethyl sulphoxide]. *J. Chem. Soc. Dalton Trans*., 1991, **1991**, 2145–2152.
30. Casellato, U., Cuerriero, P., Tamburini, S. and Vigato, P., Mononuclear, homo- and heteropolynuclear complexes with acyclic compartmental schiff bases. *Inorg. Chim. Acta*., 1993, **207**, 39–58.
31. Sakamoto, M., Nishida, Y., Matsumoto, A., Sadaoka, Y., Sakai, M., Fukuda, Y., Ohba, M., Sakiyama, H., Matsumoto, N. and Okawa, N., Nickel(II)-lanthanide(III) complexes of the dinucleating ligand N,N′-bis(3-hydroxysalicylidene)ethylenediamine. *J. Coord. Chem*., 1996, **38**, 347–354.
32. Ladavos, A. K., Kooli, F., Moreno, S., Skaribas, S. P., Pomonis, P. J., Jones, W. and Poncelet, G., Characterization and catalytic activity of La_yMO_x (M = Ni, Co) perovskite-type particles intercalated in clay via heterobinuclear complexes. *Appl. Clay Sci*., 1998, **13**, 49–63.
33. Martínez-lope, M. J. and Alonso, J. A., Thermal stability of rare-earth nickelates. Part I: the $RNiO_3$ (R = La, Pr, Nd, Sm, Eu) perovskite. *Eur. J. Solid State Inorg. Chem*., 1995, **32**, 363–371.
34. Nakamura, T., Petzow, G. and Gauckler, L. J., Stability of the perovskite phase $LaBO_3$ (B = V, Cr, Mn, Fe, Co, Ni) in reducing atmosphere. *Mat. Res. Bull*., 1979, **14**, 649–659.
35. Shannon, R. D., Revised effective ionic radii and systematic studies of interatomic distances in halides and chalcogenides. *Acta. Cryst*., 1996, **A32**, 751–767.
36. Johnson, D. W. Jr, Gallagher, P. K., Schrey, F. and Rhodes, W. W., Preparation of high surface area substitued catalysts. *Ceram. Bull*., 1976, **55**(5), 520–527.
37. Shimizu, Y. and Egashira, M., Basic aspects and challenges of semiconductor gas sensors. *MRS Bull*., 1999, **24**(6), 18–24.
38. Martinelli, G., Carotta, M. C., Traversa, E. and Ghiotti, G., Thick-film gas sensors based on nano-sized semiconducting oxide powders. *MRS Bull*., 1999, **24**(6), 30–36.